Analysis of D Pellet Injection Experiments in the W7-AS Stellarator

J. F. Lyon and L. R. Baylor, *Oak Ridge National Laboratory, Oak Ridge, TN, 37831 U.S.A.*
J. Baldzuhn, S. Fiedler, M. Hirsch, G. Kühner, and A. Weller,
Max-Planck-Institut für Plasmaphysik, EURATOM Association, 85748 Garching, Germany

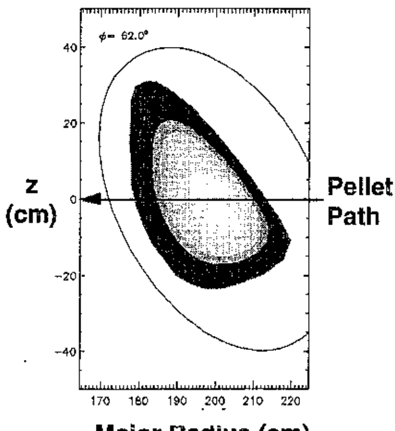

Fig.1. Typical flux surfaces and the pellet injection path in W7-AS.

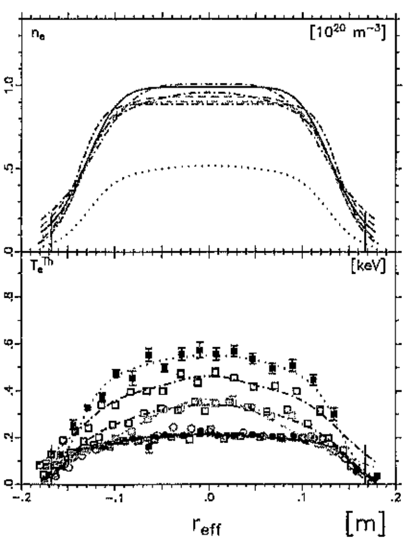

Fig. 2. Thomson scattering profiles from before pellet injection (highest T_e, lowest n_e curves) to 18.5 ms after the pellet (second highest T_e curve).

A centrifugal injector was used to inject deuterium pellets (with 3–5 × 10^{19} atoms) at ≈600 m/s into currentless, nearly shearless plasmas in the Wendelstein 7-AS (W7-AS) stellarator. The D pellet was injected horizontally at a location where the noncircular and nonaxisymmetric plasma cross section is nearly triangular (Fig. 1.) Visible-light TV pictures usually showed the pellet as a single ablating mass in the plasma, although the pellet occasionally broke in two or splintered into a cloud of small particles.

Density Evolution Following Pellet Injection in W7-AS

Figure 2 shows Thomson scattering profiles for the electron density n_e and temperature T_e immediately before and at times shortly after pellet injection (at 0.4 ms, 0.5 ms, 0.65 ms, 5.7 ms, 7.6 ms, and 18.5 ms) for a neutral-beam-heated plasma. Pellet injection leads to a rapid (< 400-μs) rise in n_e in the main part of the plasma and to a slow increase in the plasma edge on a longer (>20-ms) timescale. Microwave reflectometer measurements of the time delay (which reflects the density gradient) and FIR interferometer measurements of the line-average density also indicate that the density rises in <500 μs (Fig. 3) and then remains unchanged. The same behavior is seen in the soft X-ray intensity profiles in Fig. 4 (with 1.4 ms between curves); this signal is more influenced by density than by temperature because there was no

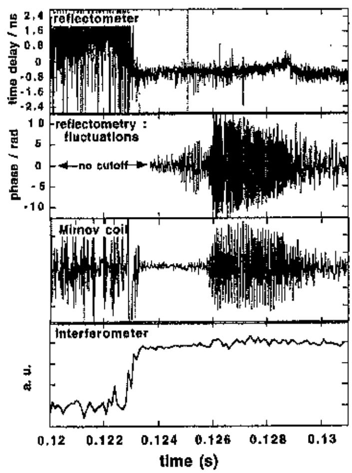

Fig. 3. Time delay and fluctuation level from a microwave reflectometer, MHD oscillations from a Mirnov coil, and line-average density around the time of pellet injection.

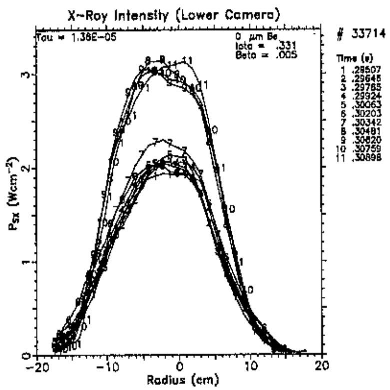

Fig. 4. Soft X-ray intensity profiles from 6.5 ms before pellet injection to 8.4 ms after a pellet.

filter in front of the soft X-ray diode array. Neutral lithium beam measurements of n_e at radii $r > 12.5$ cm (Fig. 5) show that the outer density rises slowly after pellet injection (on a 60-ms timescale), presumably due to recycling from the wall. The increase in n_e decreases with distance into the plasma.

Pellet ablation calculations using the standard neutral gas shielding model and the $n_e(r)$ and $T_e(r)$ profiles before injection indicate that the increment in density should be peaked. However, this is not seen in W7-AS on the timescale of any of the measurements. The change in the $n_e(r)$ profile in Fig. 2 is not diffusive. If it were, then the particle diffusivity would have to increase by a factor of >100 for a relatively short time (<400 μs, about the transit time for the pellet through the plasma). There was not a significant loss of injected particles during the fast density change: comparing the number of particles in the pellet with the increase in the number in the plasma after pellet injection indicates that >60% of the pellet is retained in the plasma for times >20 ms. This behavior, where the density profile after pellet injection assumes the shape of the preexisting profile without significant loss, is not seen in tokamaks. Either the ablation model is not correct and the deposition profile is the same as the initial density profile for different initial densities and field values, or a fast density redistribution occurs in these experiments in W7-AS.

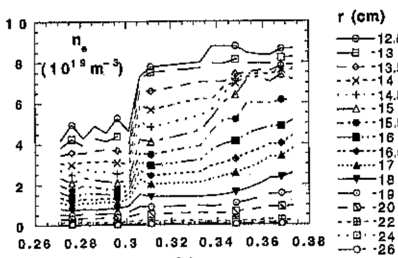

Fig. 5. Increase in the plasma density in the edge region from 30 ms before to 70 ms after a pellet.

Effect of Pellet Injection on Energy Confinement and Fluctuations in W7-AS

Figure 2 shows a rapid drop in T_e after pellet injection because the stored energy W does not change immediately. Although the $n_e(r)$ profile remains at the new (higher) value for the duration of the discharge following pellet injection, $T_e(r)$ gradually returns toward its preinjection value, indicating an increase in the energy confinement time τ_E. This is illustrated in Fig. 6 where W and τ_E increased by a factor of 2.7 for a factor of 1.7 increase in n_e. From the W7-AS τ_E scaling expression [1] $W = P\tau_E^{W7\text{-}AS} \propto n_e^{0.5}P^{0.46}$, the increase in n_e should lead to a factor of ≈1.3 increase in the stored energy because $P = P_{absorbed}$ is approximately constant at the densities in these experiments. The additional factor of 2 improvement in τ_E is due to an increase in confinement: $\tau_E/\tau_E^{W7\text{-}AS}$ is 0.7 before the pellet and 1.4 afterward. In Fig. 2, the confinement improvement (1.35) is less: $\tau_E/\tau_E^{W7\text{-}AS}$ was 0.8 before the pellet and 1.1 afterward.

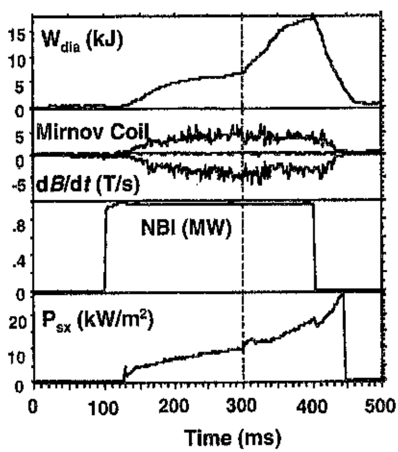

Fig. 6. Response of the plasma to pellet injection at t = 300 ms.

A few-ms quiescent period is sometimes seen in the MHD signals on Mirnov coils following pellet injection when the stored energy starts to increase, as seen in Fig. 3. In all cases, the Mirnov loop signal (often associated with degraded confinement) is reduced, and $\tau_E/\tau_E^{W7\text{-}AS}$ is >1 after a pellet. Low density fluctuation levels, followed by a decaying high-frequency burst in several discharges, were seen with the microwave reflectometer after the rapid density rise (Fig. 3). These oscillations are correlated with the Mirnov coil signal. An example of pellet injection suppressing MHD activity for a longer period with a resultant increase in τ_E is shown in Fig. 7. Without the pellet, the MHD activity and the associated enhanced energy loss persist for a longer time. It is thought that the pellet rapidly depletes the fast particle population that drives the instability [2].

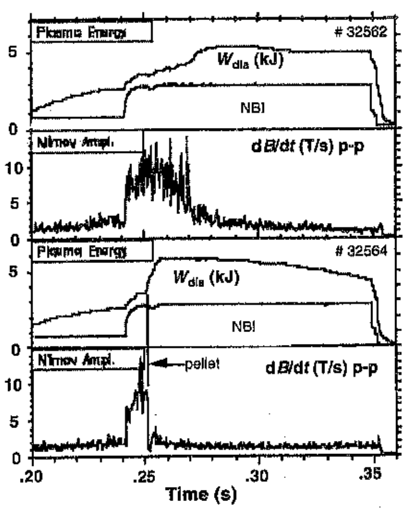

Fig. 7. MHD activity that retards transition to a high-β phase (2 top traces) is suppressed by pellet injection (2 bottom traces).

The soft X-ray (and MHD loop) signals in Fig. 8 show short-duration oscillations (for ≈300 μs) immediately after pellet injection, followed by slow (650-Hz) oscillations that damp out after a few ms and are in phase across the plasma ($m = 0$). The phase velocity of the slow oscillations indicates a disturbance propagating outward at 350 m/s. The initial burst is coincident with the fast change in n_e in the bulk of the plasma seen in Fig. 2. If the rapid change in $n_e(r)$ is due to a fast density relaxation rather than an anomalous particle deposition profile, then this burst may be evidence of an instability that causes the fast radial spreading of the high-β pellet blob. The magnetic field has low shear, a relatively weak radial gradient along the pellet path, and stronger field regions some distance toroidally on either side, which may allow a radial mixing to occur. The process may be different than in tokamaks because of the low $B \times \nabla B$ radial drift in W7-AS. In earlier experiments in W7-AS [3], the density profile became more peaked, and soft X-ray tomographic reconstruction showed small-amplitude (≈2-mm) internal oscillations in the location of the peak of the soft X-ray emission following pellet injection. In that case, the soft X-ray oscillations showed a different ($m = 1$) mode structure. Experiments with higher shear and the opposite toroidal variation of the magnetic field strength are needed to understand these observations.

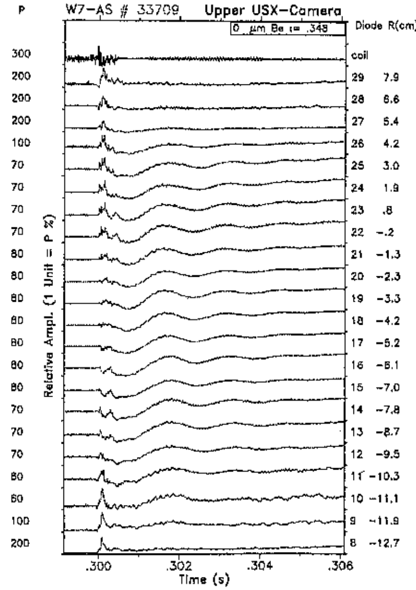

Fig. 8. Damped soft X-ray intensity oscillations following pellet injection.

The next steps involve use of a one-dimensional transport code to model the evolution of the density profile and experiments with a more versatile gas gun that allows injection with a larger range of pellet masses. Improved diagnostics — Thomson scattering triggered by the pellet, fast multichannel ECE and microwave and FIR interferometers, a Cotton-Mouton-effect polarimeter, an extensive soft X-ray array that surrounds the plasma poloidally, improved MHD loop arrays — should allow better study of the evolution of $n_e(r)$ and the associated transport.

References

[1] U. Stroth et al., *Nucl. Fusion* **36**, 1063 (1996).
[2] Max-Planck-Institut für Plasmaphysik, *IPP Annual Report 1995*, p. 59.
[3] A. Weller et al., *17th EPS Conf. on Controlled Fusion and Plasma Heating, Amsterdam*, Part II, 479 (1990).

*Research sponsored in part by the Office of Fusion Energy Sciences, U. S. Department of Energy, under contract DE-AC05-96OR22464 with Lockheed Martin Energy Research Corp.